ELSEVIER

Journal of Molecular Catalysis A: Chemical 141 (1999) 129–137

JOURNAL OF MOLECULAR CATALYSIS A: CHEMICAL

X-ray photoemission electron microscopy (XPEEM) as a new promising tool for the real-time chemical imaging of active surfaces

Y. Yamaguchi [a], S. Takakusagi [a], Y. Sakai [b], M. Kato [b], K. Asakura [c], Y. Iwasawa [a,*]

[a] *Department of Chemistry, Graduate School of Science, The University of Tokyo, Bunkyo-ku, Hongo, Tokyo 113-0033, Japan*
[b] *JEOL, 1-2 Musashino 3-chome, Akishima, Tokyo 196-0021, Japan*
[c] *Research Center for Spectrochemistry, Graduate School of Science, The University of Tokyo, Bunkyo-ku, Hongo, Tokyo 113-0033, Japan*

Abstract

We have developed a XPEEM (X-ray photoemission electron microscopy) for a new surface imaging. XPEEM is a PEEM using X-ray as an excitation source and installed with an energy filter to select an X-ray photoelectron peak specific to the target atoms. XPEEM can image the distribution of elements, chemical states and chemical species at the working surface in a mesoscopic scale.

Keywords: XPEEM; Surface imaging; Real time

1. Introduction

In catalytic and surface chemical reactions, adsorbed atoms and molecules not only act as reactants but also modify the structure and the electronic state of the surface under the working conditions and hence the reaction kinetics and mechanisms may be largely affected by coadsorbates, where the coadsorbates can activate strong adsorbates and control their reactivity and behavior [1]. It has been reported the decomposition path of HCOOH adsorbed on a $TiO_2(110)$ surface depends on the presence of HCOOH in the gas phase [2]. When no HCOOH was present in the gas phase, the surface HCOOH was converted to $CO + H_2O$ by a unimolecular reaction. The gas phase HCOOH molecules promoted a bimolecular reaction, by which the surface HCOOH was converted to $CO_2 + H_2$. Thus gas phase molecules switch the reaction paths at the surface [2]. The switchover of reaction paths has also been observed with a Nb monomer catalyst [3]. Nb monomer attached to SiO_2 selectively converts C_2H_5OH to $CH_3CHO + H_2$ by the assist of weakly adsorbed second C_2H_5OH molecules, whereas C_2H_5OH on the Nb monomer is decomposed to $C_2H_4 + H_2O$ under vacuum [3]. Surface catalytic reactions assisted by gas phase molecules have been demonstrated to be observed in many catalytic systems, presenting an important feature [4]. The desorption of CO from a Pd polycrystalline surface is also enhanced by the adsorption [5].

* Corresponding author. Fax: +81-3-3814-2627; E-mail: iwasawa@chem.s.u-tokyo.ac.jp

1381-1169/99/$ - see front matter
PII: S1381-1169(98)00256-8

Hence characterization of active surfaces has to be done in the *presence of gas phase*. IR spectroscopy is most widely used as an in-situ characterization technique and can provide the information about adsorbates and the dynamic behavior of the adsorbates with aid of stable isotopes. However, IR does not give anything about the structure of surfaces. Substrate structures often change during the course of reactions which has been monitored by in-situ EXAFS (extended X-ray absorption fine structure) [6]. EXAFS studies revealed that the structures of active sites at catalyst surfaces changed dynamically during catalytic reactions and upon the adsorption and desorption of gases and the surface reactions were promoted in conjunction with the change of surface structures [7–14]. The supported Rh_2 dimers derived from *trans*-$(RhCp*CH_3)_2(\mu\text{-}CH_2)_2$ show high activity and selectivity for ethene hydroformylation reaction at low pressure (40.0 kPa, 413 K) [10]. It was found by in-situ IR and EXAFS experiments that CO insertion as a key step for the catalysis is assisted by the formation of the Rh–Rh metal bonding [9,11].

These in-situ studies are valid for the surfaces where reactions proceed homogeneously, because they present spatially averaged characters. However, real catalyses occur inhomogeneously on the catalyst surfaces and synergistic effects between different domains may play an important role in catalytic performance. Pt/Al_2O_3 is known as a reforming catalyst, where Pt particles provide the dehydrogenation sites and acidic sites of Al_2O_3 catalyze isomerization reactions [15]. The concept 'remote-control' has been proposed for the selective oxidation of hydrocarbons on mixed oxides [16]. In this theory, two or more sites share the catalyses, activating oxygen and hydrocarbons independently and the selective catalysis depends on the inhomogeneity of the surface composition [17]. Moreover, adsorption and reaction on single crystals also occur inhomogeneously, especially in two-component reactions. CO and oxygen adsorbed on Pt(110) form their domains randomly and the size and shape of the domains change continuously during the oxidation reaction [18].

Consequently, a spatial-resolved method under in-situ conditions is prerequisite for the characterization of catalysts as the next stage. Recent progress in microscopy enables one to obtain 'real-time' surface imaging. SPM (scanning probe microscopy) such as STM and AFM is among the most important techniques for surface imaging [19]. Our knowledge about catalysts and surfaces on an atomic and molecular scale has expanded by visualizing the movement of single atoms or single molecule [20,21]. However, a disadvantage of these techniques is that they cannot easily give the chemical information such as the identification of molecules and atoms. PEEM (photoemission electron microscopy) is a microscopy to provide surface mesoscopic images by ejected photoelectrons [18]. In-situ study of working surfaces by PEEM is possible under low pressure conditions. When an X-ray is used as a source for excitation of inner-level electrons and a photoelectron peak is selected using an energy filter, one can obtain the surface imaging reflecting the distribution of selected element or its chemical state. In this paper we will discuss the possibility and advantage of XPEEM (X-ray photoemission electron microscopy) as a new real time chemical imaging method for the study of inhomogeneous catalyst surfaces related to practical catalysts.

2. Surface imaging by PEEM

When a sample is irradiated by the photon with an energy ($h\nu$) higher than the work function (ϕ), photoelectrons are ejected from the surface. The number of the emitted photoelectrons, I, is described by Eq. (1)

$$I \propto (h\nu - e\phi)^2, \tag{1}$$

where e is a charge of electron. When the photoelectrons are collected by electron lens on a screen, the surface image reflecting the distri-

bution of work function is obtained. Namely, the part of the surface with a smaller work function appears brighter. Such an image technique is called as PEEM [18]. Engel et al. have developed an UHV flange-compatible compact PEEM system [22]. Work functions vary with the materials and the mirror index of exposed surfaces. For example, the work functions of Au(100), Au(110) and Au(111) are 5.47, 5.37, and 5.31 eV, respectively, and those of Pt(100) and Pt(111) are 5.84 and 5.93 eV, respectively. Work functions also change by gas adsorption. When CO and O_2 adsorb on the Pt surfaces, the work functions increase by 0.3 and 1.0 eV, respectively. Thus the distribution of atoms or domains with different surface structures can be imaged by PEEM. The contrast in PEEM image is most enhanced when the excitation photon energy is properly adjusted at the middle of the work functions of the surface domains which one wants to distinguish from each other. When a Pt(100) surface is illuminated by a D_2 discharge lamp (cutoff energy 6.7 eV, a little larger than the work function of the clean Pt surface), the brightness in PEEM image decreases in the order, clean Pt surface > CO adsorbed domain > oxygen adsorbed domain. PEEM is a technique to provide a 'real time' imaging of surface under in-situ conditions. Since there is a small aperture between the microscope part and the sample, gas dose up to 10^{-3}–10^{-4} mbar is possible while one can maintain a high vacuum level in the microscope chamber using differential pumping. This point is important to carry out in-situ imaging experiments under reaction conditions. A typical spatial resolution of the PEEM system is about 100 nm.

2.1. Application of PEEM to surface phenomena

PEEM can monitor the diffusion process of adsorbates and the growth process of surface species. The CO diffusion coefficient on Pt(110) was determined to be 1×10^{-7} cm^2/s by a combination of PEEM and a laser induced thermal desorption [23,24]. PEEM was applied to the oxidation and dissolution processes of chemical vapor deposited carbon films on Mo substrate with good contrast [25].

PEEM is used as an in-situ monitor for the preparation of a new surface materials. Subsurface oxygen on Pt is usually produced at high temperatures like 800 K with high oxygen pressures. When the growth of oxygen domains was carefully controlled by measuring the PEEM image to attain an appropriate size on a CO-precovered Pt(100) surface at 400 K, subsurface oxygen was produced by heating the sample to 500 K under UHV conditions [26,27]. The formation of the subsurface oxygen is unique because it does not require high pressure of oxygen and high temperature but it requires an optimal size of the oxygen domain.

Rotermund et al. investigated the dynamic behavior of adsorbed CO and oxygen during CO-oxidation reactions on Pt(100) and Pt(110) by PEEM [28,29]. The CO oxidation reaction on Pt(100) and Pt(110) surface is known to exhibit the oscillatory behavior in the reaction rate under the steady-state conditions [30]. They found the spatial–temporal patterns of adsorbed CO and oxygen. These patterns formed on the surface were travelling waves, domain growths, target patterns, spiral patterns, chemical turbulences and so on, depending on the reaction conditions and crystal surfaces [18]. Gottschalk et al. reported a unique rectangular-shape target pattern in the $NO + H_2$ reactions [31]. These examples indicated that surface reactions do not always occur homogeneously even on single crystal surfaces and the reactions on different domains at a surface can interact with each other over the range of micrometers through diffusion.

2.2. PEEM investigation of reactions on composite surfaces

As mentioned in Section 1, real catalysts are composed of two or more components which may make heterogeneous domains and the syn-

ergistic behavior of the different active sites may control the selectivity of catalysts. Recently well-defined inhomogeneous surfaces have been produced by vacuum evaporation of metals and by the lithographies. Zuburtikudis and Saltsburg prepared linear metal nanocluster using vacuum-deposition and lithography [32]. They produced model Ni/SiO_2 catalysts by making alternating Ni and SiO_2 layers on a 3-in. Si wafer. On the model catalyst the C_2H_6 hydrogenolysis to form CH_4 was carried out and the rate was a maximum at Ni thickness of 3.0 nm. Ribeiro and Somorjai [33] and Jacobs et al. [34] produced the Pt arrays with 50 nm diameter and 15 nm height with a 200 nm-spacing on oxidized silicon wafer using electron beam lithography. They studied ethene hydrogenation activity of the array surface and found a comparable activity with those of a single crystal Pt surface and on dispersed Pt particles. Pd and Pd–Au bimetallic array catalysts were also produced on the SiO_2 layers obtained by oxidizing n-type Si(100) by lithography and characterized by a hydrogenation reaction [35,36].

PEEM has been applied to inhomogeneous surfaces to see how surface reactions on polycrystalline Pt undergo. Each domain has spatiotemporal patterns independently and the coupling through surface diffusion was not observed because of a large domain wall [37]. But the reaction between different domains could be sometimes coupled through the gas phase to give the oscillatory behavior [38]. The patterns on each domain are correlated to those of low-index single crystals. The partially Au-deposited Pt(110) and Pt(100) surfaces were prepared on which the propagation of reaction diffusion patterns were investigated by PEEM [39–41]. The oxygen sticking coefficient and diffusion rate of CO decreased and the propagation speed and shape of the reaction diffusion pattern changed on the Au-deposited Pt surface. The pattern formation on Pt(111) partially covered Cu was also monitored and it was concluded that the Cu domains acts as the triggering site for reaction initiation and as the modifier for the rate of reaction front propagation [42,43].

The fabricated surfaces were also studied by PEEM. The TiO_2 and Pd thick layers deposited on Pt(110) were patterned using a lithography technique [44–46]. The TiO_2 plays a role of only the wall to hinder the diffusion of adsorbates and to isolate the reaction inside the Pt surrounded by the TiO_2. Consequently a variety of new reaction–diffusion patterns have been observed by PEEM. The observations were reproduced by the theoretical simulations [47–49]. In the case of a Pd-deposited Pt(110) surface the Pd domain worked as a reservoir of CO for the adjacent Pt region [46].

3. Development of XPEEM

The PEEM cannot provide chemical information on the kind and chemical state of element on the surface. Therefore, it is difficult to clarify the surface phenomena involving chemical processes if several reactants and products coexist. XPEEM has been developed to distinguish the elements on surfaces by using the photoemission of core shell electrons which have a binding energy specific to the atom. There are two types of XPEEM. One is to use a tunable X-ray source and the other is to use an energy filter.

In the former method two PEEM pictures are measured with two different photon energies, i.e., just before and just after the X-ray absorption edge. The pictures are subtracted between them. The amount of the electrons before absorption edge coming from the atoms at issue is small but after the edge, it becomes much larger. Thus the domain containing the atoms at issue becomes brighter in the different photon energy pictures but the other shows no difference. This technique requires the tunable X-ray source like synchrotron radiation. Tonner et al. prepared Au overlayer (100 nm thick) on Si substrate [50]. The image at 108 eV photon energy for Au overlayer is brighter than that for Si substrate because the Au $4f_{7/2}$ binding energy was about

78 eV less than the photon energy used. When the photon energy was less than the Au 4f threshold energy ($h\nu = 45$ eV), the Au region became darker than the Si substrate. Stöhr et al. reported the imaging photoelectron microscopy using circularly polarized soft X-rays. They measured magnetic circular X-ray dichroism (MCXD) of magnetic domains on a CoPtCr magnetic recording disk [51]. In the MCXD spectra of Co $L_{2,3}$ edge, the intensities of L_3 edge varied when the photon spin changed from parallel to antiparallel alignment against magnetization vectors of the materials. At the same time the intensities of L_2 edge also changed reversely. Consequently the magnetic domains were contrasted according to the magnetization vectors and the intensities were inverted when the sample was imaged at L_3 and L_2 edges.

The other type of XPEEM uses an energy selection filter [52–56]. In this case an in-lab X-ray source using constant X-ray energy is available. By adopting a Wien filter, the energy filter can be installed coaxially on the PEEM optics to make the adjustment easier. In the Wien filter, the electric field and magnetic field are applied to electrons perpendicularly in the electron propagation direction as shown in Fig. 1 [56]. Therefore, the electron can go straight when the following equation is satisfied.

$$E_1^x(Z) = \nu B_1^y(Z) \tag{2}$$

where E_1^x and B_1^y are x component of electric field and y component of magnetic field, respectively. For the slower or faster electrons are bent up and down and the energy dispersion occurs after the Wien filter. In order to obtain a real time image, the Wien filter should have the lens function. This is achieved by including the quadrupole of electronic and magnetic fields [55].

Fig. 2 shows the XPEEM system that we have developed [56]. The instrument was originally produced as a LEEM/MEEM measurement system [54]. By installing a deuterium lamp and an X-ray source, PEEM and XPEEM

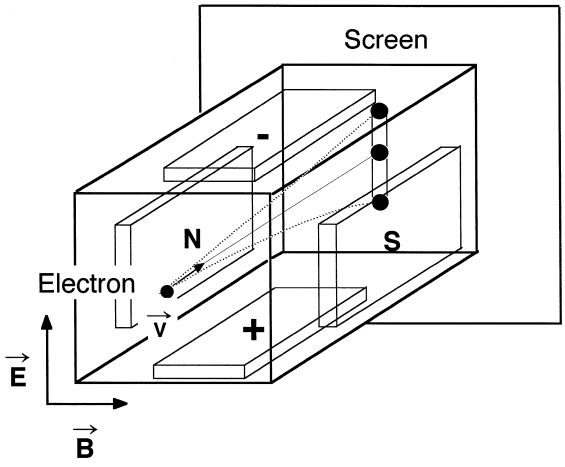

Fig. 1. Schematic view for the principle of Wien filter. Electron coming from the left side with velocity v goes straight when Eq. (2) is satisfied. Otherwise the electron is bent up or down according to its velocity.

observations became possible. Al–Kα was used as an X-ray source which was monochromatized and focused on a sample. The X-ray source and a sample chamber are separated by an Al window and the X-ray source is evacuated by an ion-pump independently.

Excited electrons are accelerated and collected by the 3-electrode cathode objective lens by applying 10 kV on the sample. Comparing to 2-electrode cathode objective lens, a high spatial resolution is generally achieved by the 3-electrode cathode objective lens but the discharge tends to occur due to the higher voltage applied between the sample and the lens. The first and third electrodes are grounded and the focusing condition is satisfied by changing voltage of the second electrode. The beam separator (BSE) is located after the cathode objective lens, where the incident electrons from an electron gun (placed at the upper side of the optical axis to measure LEEM) are bent toward the sample and the emitted one from the sample travels straightly on the optical axis by applying the electric and magnetic fields perpendicularly to each other. Because the emitted electrons are always on the optical axis, the adjustment of microscope is easily carried out.

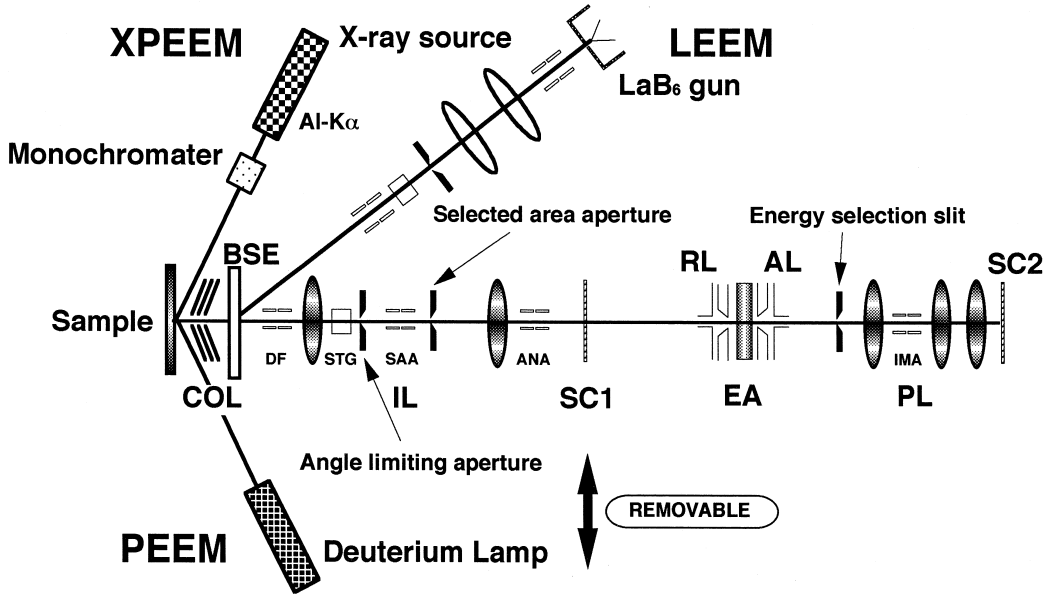

Fig. 2. Diagram of XPEEM system. COL: cathode objective lens, BSE:beam separator, IL: intermediate lens, SC1: screen 1, RL: retardation lens, EA: Wien filter, AL: acceleration lens, PL: project lens, SC2: screen 2.

The electron then propagates through an intermediate lens system which are composed of magnetic lenses. One can observe a surface image of energy-unselected electrons on the removable screen (SC1). The electrons then enter the Wien filter as mentioned above. The photoelectrons are first decelerated by the retardation lens to 200 eV. Consequently, we can accomplish an energy resolution of 0.6 eV in the Wien filter. The electrons with an appropriate kinetic energy are selected to be imaged on

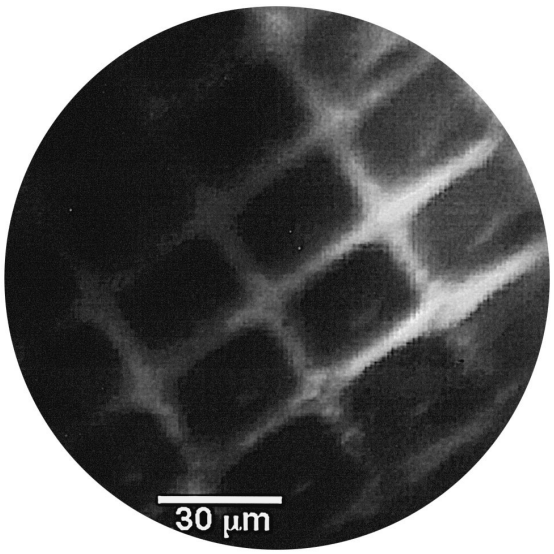

Fig. 3. PEEM picture of the Ag-deposited Cu mesh using a deuterium lamp. The scale was given in the figure. The accumulation time is 1 s.

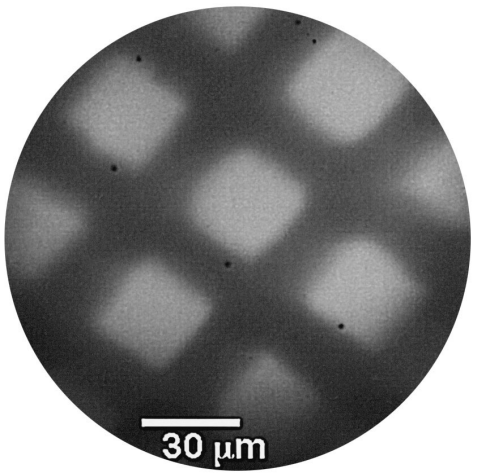

Fig. 4. XPEEM picture of Au island on a Si(111) surface. Al–Kα radiation was used. The picture was taken with 10 s exposure.

the final screen (SC2) by changing the voltage of the retardation lens and the energy selection slit. The electrons are accelerated to the original speed by the acceleration lens (AL) after the Wien filter. The electrons which can go through the energy selection slit are used to make an image on the screen (SC2).

Fig. 3 shows a PEEM picture of the Ag-deposited Cu mesh using a deuterium lamp. The 30 μm-separated mesh pattern was imaged on the screen after the accumulation of the electrons for 1 s. The spatial resolution was about 0.1 μm. Fig. 4 shows a XPEEM picture of 10 nm thick Au island on a Si(111) surface, where the Wien filter was not operated and the total electrons, mainly secondary electrons with low kinetic energies, were used for the imaging. The picture of Fig. 4 was recorded with 10 s exposure and its spatial resolution was around 10 μm due to the chromatic abbreviation. Fig. 5 shows the energy dispersion image around Au 4f photoelectrons coming from the Au island on Si(111) sample. The Wien filter was operated and the electrons were distributed linearly according to the kinetic energies as shown in Fig. 1. The picture was accumulated for 10 min using a Peltier-cooling CCD camera. By searching better optical conditions and using a liq. N_2-cooling CCD camera, we will obtain the energy filtering image.

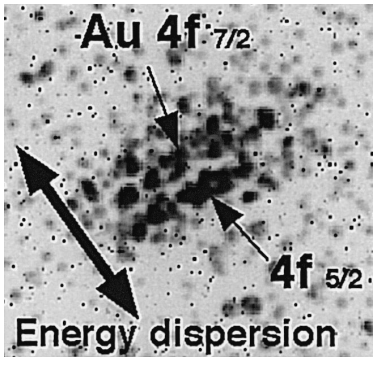

Fig. 5. The energy dispersion image around Au 4f photoelectrons coming from the Au island on Si(111) sample shown in Fig. 4. The image was accumulated for 10 min.

4. Discussion

Spatial resolution of LEEM/XPEEM can be written as

$$d^2 = d_D^2 + d_s^2 + d_c^2 \quad (3)$$

where the diffraction aberration $d_D = 0.61\lambda_0/\alpha_0$, spherical aberration, $d_s = 1/2C_s i\alpha_0^3$, chromatic aberration $d_c = C\Delta E/E_0)\alpha_0$, C_s and C_c are spherical and chromatic aberration coefficients, respectively. λ_0 and E_0 are the wavelength and the kinetic energy at the object plane. α_0 is an extraction angle of the photoelectrons from the sample. In the energy selective XPEEM, the chromatic aberration decreases because of smaller $\Delta E/E_0$, but the extraction angle of the photoelectrons from the sample should be increased to bring more electrons into the microscope. Thus the overall resolution is estimated to be about 1–10 μm. Improvement of the X-ray source increases the time and spatial resolutions. The maximum spatial resolution is calculated to be about 10 nm when we choose the optimal α_0 [55]. Synchrotron radiation is one of the possible X-ray sources but it requires a large facility. Although a smaller synchrotron radiation source using superconducting magnets has been developed, it is not applied to in-lab scale experiment. Plasma X-ray may be preferable as an in-lab XPEEM source [57].

The features of the XPEEM that we have developed are summarized as follows.

1. spatial resolution of micrometer order
2. in-situ measurement
3. element discrimination imaging
4. small sample damage

Analytical TEM has also been applied to obtain the element distribution where electrons are focused on the sample and X-ray fluorescence excited by the electron is measured. The resolution of the analytical TEM is several nm. In-situ TEM has been developed using an environmental cell with pinholes [58]. This cell enables one to measure TEM images at 2 Torr for hydrogen and 15 Torr oxygen. The disadvan-

tage of TEM is to damage the sample, especially the adsorbed system by using the high energy electron.

STM and AFM have made rapid progress in the last decade. They can resolve individual atoms and molecules on metal, semiconductors and metal oxide surfaces. The merit of these microscopies is that they can be operated in any conditions such as in the vacuum, liquid phase and ambient gas. Recently in-situ measurements at high temperature have been performed with STM [59,60]. The adsorbates such as HCOOH and pyridine on TiO_2(110) have also been resolved by STM [61,62]. But STM and AFM is that they can hardly tell chemical information of the observed images. The XPEEM method has great advantage for the observation of dynamic chemical phenomena at surfaces such as adsorption, diffusion and structure sensitive reactions. Thus new applications of XPEEM to mesoscopic processes are under investigation.

Acknowledgements

The work is partially supported by a Grant-in-Aid for Scientific Research on Priority Areas ('Functionally Graded Materials' under Contract No. 09229218 by the Ministry of Education, Science, Sports and Culture Government of Japan) and by CREST (Core Research for Evolutional Science and technology)of JST (the Japan Science and Technology).

References

[1] Y. Iwasawa, Stud. Surf. Sci. Catal. 101 (1996) 21.
[2] H. Onishi, T. Aruga, Y. Iwasawa, J. Catal. 146 (1994) 557.
[3] M. Nishimura, K. Asakura, Y. Iwasawa, Proc. 9th Int. Congr. Catal., (1988) 1842.
[4] Y. Iwasawa, Acc. Chem. Res. 30 (1997) 103.
[5] T. Yamada, Z. Runsheng, Y. Iwasawa, K. Tamaru, Surf. Sci. 205 (1988) 82.
[6] Y. Iwasawa, Proc. 9th Int. Conf. X-ray Absorption, Fine Structure, Grenoble, 1997, C2–C67.
[7] Y. Iwasawa, K. Asakura, H. Ishii, H. Kuroda, Z. Phys. Chem. N.F. 144 (1985) 105.
[8] K. Asakura, Y. Iwasawa, Physica B 158 (1989) 152.
[9] K. Asakura, K.K. Bando, K. Isobe, H. Arakawa, Y. Iwasawa, J. Am. Chem. Soc. 112 (1990) 3242.
[10] K.K. Bando, K. Asakura, H. Arakawa, Y. Sugi, K. Isobe, Y. Iwasawa, J. Chem. Soc., Chem. Commun., 1990, 253.
[11] K. Asakura, K.K. Bando, Y. Iwasawa, H. Arakawa, K. Isobe, J. Am. Chem. Soc. 112 (1990) 9096.
[12] B.S. Clausen, L. Grabak, G. Steffensen, P.L. Hansen, H. Topsoe, Catal. Lett. 20 (1993) 23.
[13] B.S. Clausen, J. Schiotz, L. Grabaek, C.V. Ovesen, K.W. Jaconsen, J.K. Norskov, H. Topsoe, Topics Catal. 1 (1994) 367.
[14] T. Ressler, M. Hagelstein, U. Hatje, W. Metz, J. Phys. Chem. B 101 (1997) 6680.
[15] J.H. Sinfelt, Adv. Chem. Eng. 5 (1964) 37.
[16] B. Delmon, G. Froment, Catal. Rev. 38 (1996) 69.
[17] S. Albonetti, F. Cavani, F. Trifiro, Catal. Rev. 28 (1996) 413.
[18] H.H. Rotermund, Surf. Sci. Report 29 (1997) 265.
[19] S. Amelinckx, D. van Dyck, J. Van Landuyt, G. Van Tendeloo, in: Handbook of Microscopy—Applications in Materials Science, Solid-State Physics and Chemistry, Weinheim, 1997.
[20] H. Onishi, Y. Iwasawa, Langmuir 10 (1994) 4414.
[21] H. Onishi, Y. Iwasawa, Phys. Rev. Lett. 76 (1995) 791.
[22] W. Engel, M.E. Kordesch, H.H. Rotermund, S. Kubala, A. von Oertzen, Ultramicroscopy 36 (1991) 148.
[23] A. von Oertzen, H.H. Rotermund, S. Nettesheim, Chem. Phys. Lett. 199 (1992) 131.
[24] A. von Oertzen, H.H. Rotermund, S. Nettesheim, Surf. Sci. 311 (1994) 322.
[25] C. Wang, J.D. Shovlin, M.E. Kordesch, J.M. Macaultay, Diamond Rel. Mater. 3 (1994) 1066.
[26] J. Lauterbach, K. Asakura, H.H. Rotermund, Surf. Sci. 313 (1994) 52.
[27] H.H. Rotermund, J. Lauterbach, G. Haas, Appl. Phys. A 57 (1993) 507.
[28] H.H. Rotermund, W. Engel, M. Kordesch, G. Ertl, Nature 343 (1990) 355.
[29] H.H. Rotermund, S. Nettesheim, A. von Oertzen, G. Ertl, Surf. Sci. 275 (1992) L645.
[30] R. Imbihl, Prog. Surf. Sci. 44 (1993) 185.
[31] N. Gottschalk, F. Mertens, M. Bar, M. Eiswirth, R. Imbihl, Phys. Rev. Lett. 73 (1994) 3483.
[32] I. Zuburtikudis, H. Saltsburg, Science 258 (1992) 1337.
[33] F.H. Ribeiro, G.A. Somorjai, Rec. Trav. Chim. Pays-Bas. 113 (1994) 419.
[34] P.W. Jacobs, F.H. Ribeiro, G.A. Somorjai, Catal. Lett. 37 (1996) 131.
[35] A.C. Krauth, G.H. Bernstein, E.E. Wolf, Catal. Lett. 45 (1997) 177.
[36] A.C. Krauth, K.H. Lee, G.H. Bernstein, E.E. Wolf, Catal. Lett. 27 (1994) 43.
[37] J. Lauterbach, G. Haas, H.H. Rotermund, G. Ertl, Surf. Sci. 294 (1993) 116.
[38] J. Lauterbach, H.H. Rotermund, Catal. Lett. 27 (1994) 27.
[39] K. Asakura, J. Lauterbach, H.H. Rotermund, G. Ertl, Phys. Rev. B 50 (1994) 8043.
[40] K. Asakura, J. Lauterbach, H.H. Rotermund, G. Ertl, Surf. Sci. 374 (1997) 125.
[41] K. Asakura, J. Lauterbach, H.H. Rotermund, G. Ertl, J. Chem. Phys. 102 (1995) 8175.

[42] M. Kolodzejczyk, R.E.R. Colen, B. Delmon, J.H. Block, Appl. Surf. Sci. 121/122 (1996) 480.
[43] M. Kolodziejczyk, R.E.R. Colen, M. Berdau, B. Delmon, J.H. Block, Surf. Sci. 375 (1997) 235.
[44] M.D. Graham, Y.G. Kevrekidis, K. Asakura, J. Lauterbach, H.H. Rotermund, G. Ertl, Science 264 (1994) 80.
[45] M.D. Graham, M. Bär, I.G. Kevrekidis, K. Asakura, J. Lauterbach, H.H. Rotermund, G. Ertl, Phys. Rev. E 52 (1995) 76.
[46] J. Lauterbach, K. Asakura, P.B.Rasmussen, H.H. Rotermund, M. Bär, M.D. Graham, I.G. Kevrekidis, G. Ertl, J. Phys. D, to be published.
[47] M. Bär, I.G. Kevrekidis, H.H. Rotermund, G. Ertl, Phys. Rev. E 52 (1995) 5739.
[48] G. Haas, M. Bär, I.G. Kevrekidis, P.B. Rasmussen, H.H. Rotermund, G. Ertl, Phys. Rev. Lett. 75 (1995) 3560.
[49] M. Bär, S.K. Bangia, I.G. Kevrekidis, H. Haas, H.-H. Rotermund, G. Ertl, J. Phys. Chem. 100 (1996) 19106.
[50] B.P. Tonner, G.R. Harp, Rev. Sic. Instrum. 69 (1988) 853.
[51] J. Stöhr, Y. Wu, B.D. Hermsmeier, M.G. Samant, G.R. Harp, S. Koranda, D. Dunham, B.P. Tonner, Science 259 (1993) 658.
[52] G.K.L. Marx, V. Gerheim, G. Schoenhense, J. Electr. Spectrosc. 84 (1997) 251.
[53] E. Bauer, in: S. Amelinckx, D. van Dyck, J. van Landuyt, G. van Tendeloo (Eds.), Low Energy Electron Microscopy, VCH, Weinheim, 1997, 487 pp.
[54] Y. Harada, S. Yamamoto, M. Aoki, S. Masuda, T. Ichinokawa, M. Kato, Y. Sakai, Nature 372 (1994) 657.
[55] M. Kato, Theory and Design of Energy Analyzing Systems for Electron Spectroscopy, Thesis, The University of Tokyo, 1997.
[56] Y. Yamaguchi, Development of in-situ XPEEM and Real Time Imaging System, Thesis, The University of Tokyo, 1998.
[57] D. Duston, J. Davis, Phys. Rev. A 23 (1981) 2602.
[58] T.L. Neils, J.M. Burlitch, J. Catal. 118 (1989) 79.
[59] H. Onishi, K. Fukui, Y. Iwasawa, Bull. Chem. Soc. Jpn. 68 (1995) 2447.
[60] H. Onishi, Y. Yamaguchi, K. Fukui, Y. Iwasawa, J. Phys. Chem. 100 (1996) 9582.
[61] H. Onishi, Y. Iwasawa, in: M.W. Roberts (Ed.), Interfacial Chemistry on Metal Oxide Single Crystals Relevant to Oxide Catalysis, Oxford, 1997.
[62] S. Suzuki, Y. Yamaguchi, H. Onishi, K. Fukui, T. Sasaki, Y. Iwasawa, Catal. Lett., in press.